

# Through-Bond Orbital Coupling, the Parity Rule, and the Design of “Superbridges” Which Exhibit Greatly Enhanced Electronic Coupling: A Natural Bond Orbital Analysis

Michael N. Paddon-Row\* and Michael J. Shephard

Contribution from the School of Chemistry, University of New South Wales, Sydney, 2052, Australia

Received December 2, 1996. Revised Manuscript Received March 24, 1997<sup>⊗</sup>

**Abstract:** An *ab initio* molecular orbital study of through-bond (TB) orbital interactions has been carried out on several series of diene hydrocarbons, **2(n)**–**17(n)**, in which the double bonds are covalently attached to a variety of rigid saturated hydrocarbon bridges with lengths, *n*, ranging from four to 17 C–C  $\sigma$  bonds. The resulting TB  $\pi_+$ ,  $\pi_-$  and  $\pi^*_+$ ,  $\pi^*_-$  splitting energies,  $\Delta E(\pi)$  and  $\Delta E(\pi^*)$ , respectively, were obtained at the HF/3-21G level of theory. The distance dependence of  $\Delta E(\pi)$  and  $\Delta E(\pi^*)$  for each type of diene was fitted to the respective exponential decay profiles,  $\Delta E(\pi) = A \exp(-\beta_h n)$  and  $\Delta E(\pi^*) = B \exp(-\beta_e n)$ . It was found that both  $\beta_h$  and  $\beta_e$  were dependent on the nature of the hydrocarbon bridge. For example,  $\beta_h$  is found to range from 0.6 per bond for **3(n)** to only 0.05 per bond for **7(n)** and **8(n)**. The  $\beta_h$  values for the polynorbornane bridge dienes, **2(n)**, and the hybrid norbornane–bicyclo[2.2.0]hexane bridge dienes, **3(n)**, are notably larger than that for the divinylalkanes, **4(n)**, and Natural Bond Orbital (NBO) analyses revealed this to be due to destructive interference effects between the two main relays of the bridges in **2(n)** and **3(n)**. A simple intuitive model, based on the parity rule of TB coupling, was developed to explore interrelay interference effects in TB coupling along various saturated hydrocarbon bridges. The parity rule model was successfully used to design systems **5(n)**–**16(n)** in which the TB coupling between the two double bonds is greatly enhanced by *constructive* interrelay interference. For example, the absolute value for  $\Delta E(\pi)$  for the 15-bond diene **8(15)** is 0.21 eV, an extraordinarily large quantity, considering that the double bonds are 17 Å apart, and  $\beta_h$  for the series **8(n)** is only 0.05 per bond. TB coupling in the “superbridges” **7(n)**, **8(n)**, **11(n)**, **12(n)**, **15(n)**, and **16(n)** can be up to two orders of magnitude stronger than that present in **2(n)** and **3(n)**. The enhanced degree of TB coupling in the former systems translates into a predicted increase in the rate of hole transfer in the cation radicals of **7(14)** and **8(15)** of *four orders of magnitude*, compared to that for the cation radical of **3(14)**. NBO analyses of TB coupling in **5(n)** and **9(n)** revealed that strong interrelay interference may occur even when one of the relays is not electronically coupled to either double bond. It was found that the original version of the parity rule required modification so that it takes into account any change in parity of a coupling pathway caused by sign inversions between coupling orbitals. A *relative* parity rule of TB coupling is proposed which correctly addresses the topology of orbital overlap. Compared to  $\pi$ -TB coupling, TB interactions involving  $\pi^*$  orbitals are less affected by interrelay interference, constructive or destructive.

## Introduction

The concept of through-bond (TB) orbital interactions<sup>1–8</sup> is presently enjoying a resurgence of interest, largely as a result of recent experimental studies<sup>9–28</sup> which suggest that such

interactions are responsible for mediating long-range electron-transfer (ET) processes. In these processes it is believed that the electronic coupling between the donor and acceptor chromophore orbitals arises from their mutual interaction with the orbitals of the intervening medium.<sup>1–3</sup> In the most general

<sup>⊗</sup> Abstract published in *Advance ACS Abstracts*, May 1, 1997.

(1) Hoffmann, R.; Imamura, A.; Hehre, W. J. *J. Am. Chem. Soc.* **1968**, *90*, 1499.

(2) Hoffmann, R. *Acc. Chem. Res.* **1971**, *4*, 1.

(3) Paddon-Row, M. N. *Acc. Chem. Res.* **1982**, *15*, 245.

(4) Wasielewski, M. R. In *Photoinduced Electron Transfer*; Fox, M. A., Chanon, M., Eds.; Elsevier: Amsterdam, 1988; Part A.

(5) McConnell, H. M. *J. Chem. Phys.* **1961**, *35*, 508.

(6) Closs, G. L.; Miller, J. R. *Science* **1988**, *240*, 440.

(7) Gleiter, R.; Schaefer, W. *Acc. Chem. Res.* **1990**, *23*, 369.

(8) Jordan, K. D.; Paddon-Row, M. N. *Chem. Rev.* **1992**, *92*, 395.

(9) Paddon-Row, M. N. *Acc. Chem. Res.* **1994**, *27*, 18.

(10) Lawson, J. M.; Paddon-Row, M. N.; Schuddeboom, W.; Warman, J. M.; Clayton, A. H. A.; Ghiggino, K. P. *J. Phys. Chem.* **1993**, *97*, 13099.

(11) Gould, I. R.; Young, R. H.; Mueller, L. J.; Farid, S. *J. Am. Chem. Soc.* **1994**, *116*, 8176.

(12) Kumar, K.; Lin, Z.; Waldeck, D. H.; Zimmt, M. B. *J. Am. Chem. Soc.* **1996**, *118*, 243.

(13) Winkler, J. R.; Gray, H. B. *Chem. Rev.* **1992**, *92*, 369.

(14) McLendon, G.; Hake, R. *Chem. Rev.* **1992**, *92*, 481.

(15) Isied, S. S.; Ogawa, M. Y.; Wishart, J. F. *Chem. Rev.* **1992**, *92*, 381.

(16) Schanze, K. S.; Cabana, L. A. *J. Phys. Chem.* **1990**, *94*, 2740.

(17) Schanze, K. S.; Sauer, K. *J. Am. Chem. Soc.* **1988**, *110*, 1180.

(18) Joran, A. D.; Leland, B. A.; Geller, G. G.; Hopfield, J. J.; Dervan, P. B. *J. Am. Chem. Soc.* **1984**, *106*, 6090.

(19) Leyland, B. A.; Joran, A. D.; Felker, P. M.; Hopfield, J. J.; Zewail, A. H.; Dervan, P. B. *J. Phys. Chem.* **1985**, *89*, 5571.

(20) Wasielewski, M. R.; Niemczyk, M. P.; Johnson, D. G.; Svec, W. A.; Minsek, D. W. *Tetrahedron* **1989**, *45*, 4785.

(21) Stein, C. A.; Lewis, N. A.; Seitz, G. J. *J. Am. Chem. Soc.* **1982**, *104*, 2596.

(22) Calcaterra, L. T.; Closs, G. L.; Miller, J. R. *J. Am. Chem. Soc.* **1983**, *105*, 670.

(23) Miller, J. R.; Calcaterra, L. T.; Closs, G. L. *J. Am. Chem. Soc.* **1984**, *106*, 3047.

(24) Paskan, P.; Mes, G. F.; Koper, N.; Verhoeven, J. W. *J. Am. Chem. Soc.* **1985**, *107*, 5839.

(25) Oevering, H.; Paddon-Row, M. N.; Heppener, M.; Oliver, A. M.; Cotsaris, E.; Verhoeven, J. W.; Hush, N. S. *J. Am. Chem. Soc.* **1987**, *109*, 3258.

(26) Oliver, A. M.; Craig, D. C.; Paddon-Row, M. N.; Kroon, J.; Verhoeven, J. W. *Chem. Phys. Lett.* **1988**, *150*, 366.

(27) Kroon, J.; Verhoeven, J. W.; Paddon-Row, M. N.; Oliver, A. M. *Angew. Chem., Int. Ed. Engl.* **1991**, *30*, 1358.

(28) Penfield, K. W.; Miller, J. R.; Paddon-Row, M. N.; Cotsaris, E.; Oliver, A. M.; Hush, N. S. *J. Am. Chem. Soc.* **1987**, *109*, 5061.

context, the intervening medium may be a pathway comprising solvent molecules,<sup>10–12</sup> a segment of protein,<sup>13–17</sup> or a bridge that is covalently linked to the donor and acceptor groups at its termini, that is, a donor–{bridge}–acceptor (**D–B–A**) system.<sup>18–28</sup> In this paper we restrict discussion to **D–B–A** systems where the electronic coupling occurs through saturated hydrocarbon bridges.

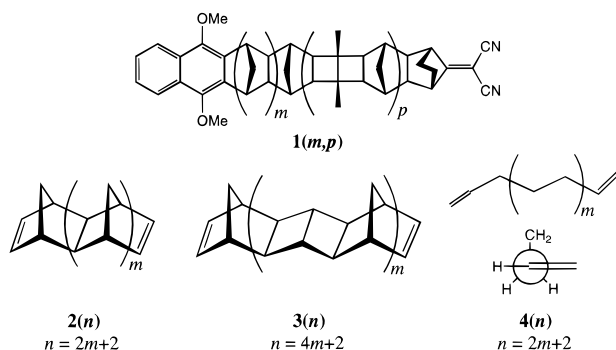
Through-bond coupling enters into nonadiabatic ET theory through its effect on the magnitude of the electronic coupling matrix element,  $H_e$ , which, in turn, is related to the electron transfer rate,  $k_e$ , by the Fermi Golden Rule expression<sup>29</sup>

$$k_e = \frac{4\pi^2}{h} |H_e|^2 \text{FCWD} \quad (1)$$

where FCWD is the Franck–Condon weighted density of states.

A useful way of exploring the dependence of the magnitude of  $H_e$  on such factors as the length, configuration, and chemical constitution of the bridge in a **D–B–A** system is to calculate the  $\pi$  MO splitting energies,  $\Delta E(\pi)$ , and the  $\pi^*$  MO splitting energies,  $\Delta E(\pi^*)$ , in model dienes in which the **D** and **A** chromophores are double bonds. It can be shown that, within the context of Koopmans' theorem (KT),<sup>30</sup> the calculated  $\Delta E(\pi)$  values for such dienes are proportional to the magnitude of the electronic coupling for hole transfer (HT) in the diene cation radicals, and the  $\Delta E(\pi^*)$  values are proportional to the magnitude of the electronic coupling for electron transfer in the corresponding anion radicals.<sup>31,32</sup>

For example, the distance dependence of the magnitude of TB coupling in the bichromophoric systems **1(m,p)** was successfully estimated from KT calculations on the model diene systems **2(n)** and **3(n)**.<sup>32,33</sup>



In general, the distance dependence of the calculated  $\Delta E(\pi)$  and  $\Delta E(\pi^*)$  values for a variety of bridged dienes can be fitted to an approximate exponential decay profile

$$\Delta E(\pi) = A \exp(-\beta_h n) \quad (2a)$$

$$\Delta E(\pi^*) = B \exp(-\beta_e n) \quad (2b)$$

where  $\beta_h$  and  $\beta_e$  are the attenuation coefficients (units: per bond) for hole transfer and electron transfer, respectively,<sup>32–34</sup> and  $n$  is the number of single C–C sigma bonds connecting the two double bonds along the shortest main relay in the bridge. In general, the exponential fit for the distance dependence of  $\Delta E(\pi)$

and, to a lesser extent,  $\Delta E(\pi^*)$  improves with increasing bridge length, and the associated  $\beta$  values calculated from adjacent members of the series tend toward a constant (limiting) value when  $n \geq 10$   $\sigma$  bonds.<sup>8</sup> This point is illustrated by the HF/3-21G  $\Delta E(\pi)$  and  $\Delta E(\pi^*)$  splittings and the corresponding  $\beta_h$  and  $\beta_e$  values for the three series of dienes **2(n)**–**4(n)** which are presented in Table 1.

The magnitude and distance dependence of  $\Delta E(\pi)$  for these series of dienes depend markedly on the nature of the bridge. Thus, the limiting  $\beta_h$  values for **2(n)** and **3(n)** are significantly larger than that for **4(n)**, and the magnitude of  $\Delta E(\pi)$  for a particular member from either of the former two series of dienes is smaller than that for the corresponding member of the latter series.<sup>35</sup> These results suggest that TB coupling through bridges possessing two main TB coupling relays, as in **2(n)** and **3(n)**, is *weaker* than that through a similar bridge but which possesses only one TB coupling relay, as in **4(n)**.<sup>36</sup> This is a somewhat surprising result, considering that simple perturbation theoretic arguments predict that  $\Delta E(\pi)$  for a bridge possessing two main relays should be double that for a bridge possessing a single main relay and that the  $\beta_h$  values should be the same for both bridges. However, a detailed Natural Bond Orbital (NBO) analysis<sup>37,38</sup> of TB coupling in **2(n)** and **4(n)** revealed the cause of the anomaly to lie in the structurally enforced proximity of the two main relays in **2(n)** which results in their interacting with each other in a manner that leads to attenuated TB coupling through the bridge.<sup>36</sup> Interrelay interference of this type has also been detected in a number of multirelay systems.<sup>39–41</sup> Interference effects have also been detected in proteins<sup>42</sup> and in systems where the two chromophores are connected by an unsaturated bridge.<sup>43</sup>

In this paper, we present a detailed analysis of interrelay interference effects on the magnitude and distance dependence of TB coupling in the  $\pi$  and  $\pi^*$  manifold in a variety of bridged dienes, **2(n)**, **3(n)**, and **5(n)**–**17(n)**. The most important outcome of this study has been the development of an intuitive, conceptual model, based on the parity rule of TB coupling,<sup>1–3,31,44</sup> that provides valuable qualitative insight into the origins of interrelay interference effects in TB coupling through multi-strand hydrocarbon bridges. In particular, we demonstrate how this rule can be used to design bridges in which TB coupling is enhanced by as much as two orders of magnitude.<sup>40</sup> Such “superbridges” offer considerable potential for mediating ET and HT processes over distances greatly exceeding those achieved by hydrocarbon bridges currently in use.

Following a brief section on the computational details, we address TB coupling involving filled  $\pi$  orbitals from which we develop our conceptual model. TB coupling involving virtual  $\pi^*$  orbitals is treated in a separate section as this type of coupling turns out to be less amenable to analysis than that involving  $\pi$  orbitals.

(35) See computational details section for discussion of the geometry of **4(n)**.

(36) Shephard, M. J.; Paddon-Row, M. N.; Jordan, K. D. *J. Am. Chem. Soc.* **1994**, *116*, 5328.

(37) Reed, A. E.; Weinhold, F. *J. Chem. Phys.* **1985**, *83*, 1736.

(38) Reed, A. E.; Curtiss, L. A.; Weinhold, F. *Chem. Rev.* **1988**, *88*, 899.

(39) Onuchic, J. N.; Beratan, D. N. *J. Am. Chem. Soc.* **1987**, *109*, 6771.

(40) For a preliminary account of this work, see: Shephard, M. J.; Paddon-Row, M. N. *J. Phys. Chem.* **1995**, *99*, 17497.

(41) Curtiss, L. A.; Naleway, C. A.; Miller, J. R. *J. Phys. Chem.* **1995**, *99*, 1182.

(42) Regan, J. J.; Di Bilio, A. J.; Langen, R.; Skov, L. K.; Winkler, J. R.; Gray, H. B.; Onuchic, J. N. *Chem. Biol.* **1995**, *2*, 489.

(43) Marvaud, V.; Launay, J. P.; Joachim, C. *Chem. Phys.* **1993**, *177*, 23.

(44) Verhoeven, J. W.; Pasman, P. *Tetrahedron* **1981**, *37*, 943.

(29) Marcus, R. A.; Sutin, N. *Biochim. Biophys. Acta* **1985**, *811*, 265.

(30) Koopmans, T. *Physica* **1934**, *1*, 104.

(31) Paddon-Row, M. N.; Jordan, K. D. In *Modern Models of Bonding and Delocalization*; Liebman, J. F., Greenberg, A., Eds.; VCH Publishers: New York, 1988.

(32) Paddon-Row, M. N.; Wong, S. S. *Chem. Phys. Lett.* **1990**, *167*, 432.

(33) Jordan, K. D.; Paddon-Row, M. N. *J. Phys. Chem.* **1992**, *96*, 1188.

(34) Broo, S.; Larsson, S. *Chem. Phys.* **1990**, *148*, 103.

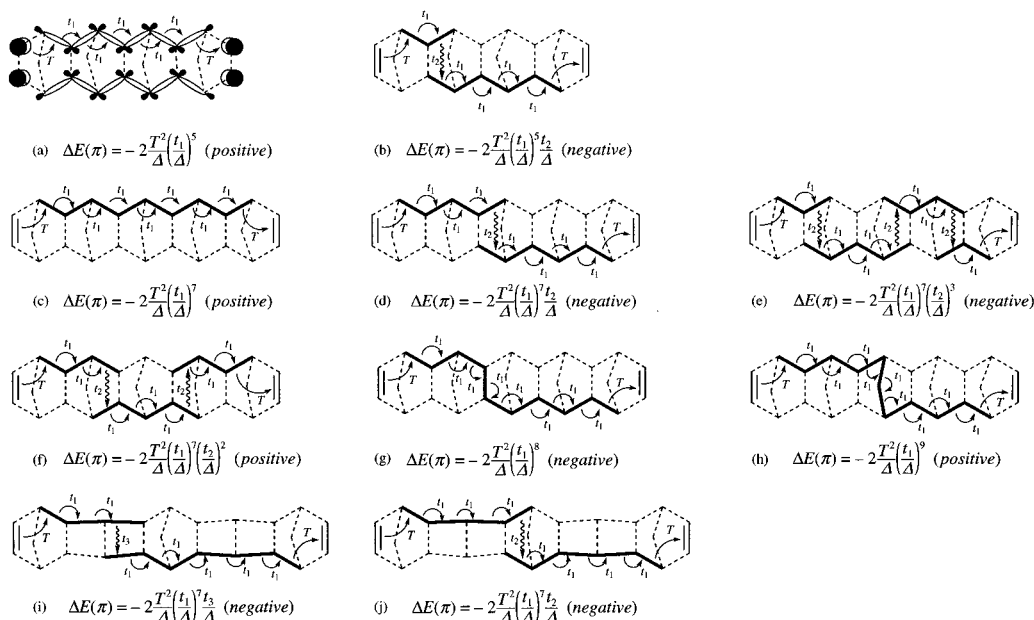


**Figure 1.** Selected  $\pi$ -TB coupling pathways (highlighted bonds) for **2(8)**, **2(10)**, and **3(10)** illustrating pathways that involve a main relay only, (a and c), pathways that include one or more through-space interrelay jumps (b, d–f, i, and j), and pathways that cross from one main relay to the other via the cross-link bonds, (g and h). The McConnell-type nearest-neighbor signed  $\Delta E(\pi)$  expressions for the pathways are also given.  $T$  is the interaction between a  $\pi$  NBO and its neighboring allylic bridge  $\sigma$  NBO;  $t_1$  is the interaction between geminal  $\sigma$  NBOs;  $t_2$  is the interaction between two facing  $\sigma$  NBOs of a norbornane bridge unit;  $t_3$  is the interaction between two  $\sigma$  facing NBOs of a bicyclo[2.2.0]hexane bridge unit; and  $\Delta$  is the energy gap between the  $\pi$  and  $\sigma$  NBOs. All  $t_1$  interactions are assumed to have the same magnitude for all pairs of  $\sigma$  NBOs; similarly all  $t_2$  interactions are assumed to be equal.

### Computational Details

The geometries of **2(n)**–**18(n)** were optimized at the HF level of theory using the STO–3G basis set.<sup>45</sup> The use of optimized geometries obtained at this level has been found to be suitable for this type of study.<sup>32,33</sup> Symmetry constraints used for the optimizations were as follows:  $C_{2v}$  symmetry for **2(n)**, **3(n)**, and **17(n)**,  $C_s$  symmetry for **5(n)**, **7(n)**, **9(n)**, **11(n)**, **13(n)**, **15(n)**, and **18(n)**, and  $C_2$  symmetry for **4(n)**, **6(n)**, **8(n)**, **10(n)**, **12(n)**, **14(n)**, and **16(n)**. In the case of the divinylalkanes, **4(n)**, the dihedral angle between the plane of each double bond and its associated allylic C–C bond was fixed at  $90^\circ$  in order to maximize the  $\pi/\sigma$  overlap. In the case of the bisbutadienylalkanes, **18(n)**, each diene unit is forced to adopt a planar, *cisoid*, geometry and the dihedral angle between the plane of each inner double bond and its associated allylic C–C bond was fixed at  $90^\circ$ .

Single point energy calculations were then carried out on each system at the (restricted) HF/3-21G level of theory<sup>46</sup> to obtain the splitting energies,  $\Delta E(\pi)$  and  $\Delta E(\pi^*)$ . Our choice of the 3-21G basis set is based on previous studies which have found that this basis set is sufficiently flexible enough to describe the TB coupling in saturated hydrocarbon bridges.<sup>33,47</sup>

The application of the NBO technique<sup>37,38</sup> for analyzing TB coupling has been described elsewhere,<sup>36,48–51</sup> and only a brief summary is given here. This technique involves the construction of a Fock matrix in the basis of localized core, lone pairs,

Ryberg-type, and two-center  $\sigma$ ,  $\sigma^*$ ,  $\pi$ , and  $\pi^*$  NBOs. The diagonal elements of the Fock matrix in the basis of the NBOs give the self-energies of the NBOs, and the off-diagonal elements give the magnitude of the interactions between pairs of NBOs.

By adding selected off-diagonal matrix elements to a “blank” Fock NBO matrix (i.e., one that only contains the diagonal elements), followed by diagonalization of the resulting matrix, one may quantitatively dissect the TB coupling into contributions from various interacting NBOs. A particularly useful aspect of the NBO method is that it provides information about interactions involving *both* filled and virtual orbital spaces, such as  $\pi/\sigma$ ,  $\pi^*/\sigma$ ,  $\pi^*/\sigma^*$ , and  $\pi/\sigma^*$  interactions.

In this study, the NBO analyses were applied to Fock NBO matrices generated from the HF/3-21G level calculations. All calculations were carried out using Gaussian 94.<sup>52</sup>

### The Parity Rule and Through-Bond Interactions Involving $\pi$ Orbitals

As mentioned in the introduction, destructive interrelay interference in **2(n)** is responsible for the inferior  $\pi$ -TB coupling in that series of dienes, compared to the  $\pi$ -TB coupling in the single chain divinylalkanes **4(n)**.<sup>36</sup> This interference arises from the interaction between the two main relays in **2(n)** which establishes additional TB coupling pathways (interrelay pathways) that either involve interrelay “jumps” (e.g., Figure 1b,d–f) or coupling through the cross-link bonds (e.g., Figure 1g,h). Such interrelay pathways may interfere either constructively or destructively with  $\pi$ -TB coupling proceeding through the main

(45) Hehre, W. J.; Stewart, R. F.; Pople, J. A. *J. Chem. Phys.* **1969**, *51*, 2657.

(46) Binkley, J. S.; Pople, J. A.; Hehre, W. J. *J. Am. Chem. Soc.* **1980**, *102*, 939.

(47) Shephard, M. J.; Paddon-Row, M. N.; Jordan, K. D. *Chem. Phys.* **1993**, *176*, 289.

(48) Paddon-Row, M. N.; Wong, S. S.; Jordan, K. D. *J. Am. Chem. Soc.* **1990**, *112*, 1710.

(49) Naleway, C. A.; Curtiss, L. A.; Miller, J. R. *J. Phys. Chem.* **1991**, *95*, 8434.

(50) Liang, C.; Newton, M. D. *J. Phys. Chem.* **1993**, *97*, 3199.

(51) Curtiss, L. A.; Naleway, C. A.; Miller, J. R. *Chem. Phys.* **1993**, *176*, 387.

(52) Frisch, M. J.; Trucks, G. W.; Schlegel, H. B.; Gill, P. M. W.; Johnson, B. G.; Robb, M. A.; Cheeseman, J. R.; Keith, T.; Petersson, G. A.; Montgomery, J. A.; Raghavachari, K.; Al-Laham, M. A.; Zakrzewski, V. G.; Ortiz, J. V.; Foresman, J. B.; Cioslowski, J.; Stefanov, B. B.; Nanayakkara, A.; Challacombe, M.; Peng, C. Y.; Ayala, P. Y.; Chen, W.; Wong, M. W.; Andres, J. L.; Replogle, E. S.; Gomperts, R.; Martin, R. L.; Fox, D. J.; Binkley, J. S.; Defrees, D. J.; Baker, J.; Stewart, J. P.; Head-Gordon, M.; Gonzalez, C.; Pople, J. A. *Gaussian 94*; Gaussian Inc.: Pittsburgh, PA.

relays. In the case of **2(n)**, the interrelay pathways that cause destructive interference (e.g., Figure 1b,d,e,g) are more important than those interrelay pathways that cause constructive interference (e.g., Figure 1f,h).

A useful and intuitive way of visualizing how these interrelay interactions affect the strength of the TB interaction energy is through application of the parity rule of TB coupling. This rule states<sup>1-3,31,44</sup> that the level ordering of two symmetry-adapted pairs of  $\pi$ -type orbitals, say  $\pi_+$  ( $= \pi_1 + \pi_2$ ) and  $\pi_-$  ( $= \pi_1 - \pi_2$ ),<sup>53</sup> arising from TB coupling with a single relay comprising  $n$  localized single bonds, depends on the parity of  $n$ , following a natural sequence, that is,  $\pi_-$  above  $\pi_+$  in energy, for even values of  $n$ , and an inverted sequence,<sup>54</sup> that is,  $\pi_+$  above  $\pi_-$ , for odd values of  $n$ . By convention, the sign of the  $\pi_+, \pi_-$  splitting energy,  $\Delta E(\pi)$ , is taken to be positive (negative) for the natural (inverted) sequence. Within the context of perturbation theory,<sup>5,8,55</sup> the overall value of  $\Delta E(\pi)$ , arising from TB coupling through  $m$  pathways of single bonds, is given by the algebraic sum

$$\Delta E(\pi) = \sum_i^m \Delta E(\pi)^i \quad (3)$$

where  $\Delta E(\pi)^i$  is the signed splitting energy (as defined above) due to coupling along the  $i$ th pathway. Applying this expression to interrelay coupling, it may be shown,<sup>56</sup> at least within the context of McConnell theory,<sup>5</sup> that interrelay pathways which have the same parity as the main relays lead to an increase in the overall value of  $\Delta E(\pi)$  and to a weaker distance dependence of  $\Delta E(\pi)$  (i.e., to a smaller  $\beta_h$  value). For this situation the main relays are said to interfere with each other constructively. On the other hand, if the interrelay pathways have opposite parity to the main relays, then coupling through these pathways leads to a decrease in the magnitude of  $\Delta E(\pi)$  and to a stronger distance dependence of  $\Delta E(\pi)$  (i.e., to a larger  $\beta_h$  value); the main relays are now said to interfere with each other destructively.

The problem of identifying those interrelay pathways that contribute most—either constructively or destructively—to the overall  $\pi$  splitting may be resolved using NBO analysis. An estimate of the importance of various TB pathways may then be made using the off-diagonal Fock NBO interaction matrix elements in conjunction with the simple McConnell second-order perturbation expression for the coupling through each pathway:<sup>5</sup>

$$\Delta E(\pi)^i = -2 \frac{T^2}{\Delta} \prod_k \frac{t_k}{\Delta} \quad (4)$$

In this expression the splitting energy,  $\Delta E(\pi)^i$ , arising from the  $i$ th pathway is the product of interactions between adjacent localized orbitals (such as NBOs) making up that pathway. In eq 4  $T$  is the interaction energy between one of the localized  $\pi$  orbitals and the respective localized  $\sigma$  or  $\sigma^*$  orbital of the relay to which it is coupled most strongly (e.g., Figure 1a),  $t_k$  is the interaction energy between two adjacent localized  $\sigma$  or  $\sigma^*$  orbitals in the pathway, the product being taken over all pairs

(53)  $\pi_+$  and  $\pi_-$  are defined in terms of their symmetry properties with respect to a symmetry operation which interchanges  $\pi_1$  and  $\pi_2$ ;  $\pi_+$  is symmetric and  $\pi_-$  is antisymmetric under this symmetry operation. For example, Figure 1a depicts the  $\pi_+$  combination in the  $C_{2v}$  symmetric diene **2(8)**.

(54) Heilbronner, E.; Schmelzer, A. *Helv. Chim. Acta* **1975**, *58*, 936.

(55) Liang, C.; Newton, M. D. *J. Phys. Chem.* **1992**, *96*, 2855.

(56) See the Appendix in ref 40.

of adjacent orbitals, and  $\Delta$  is the (average) energy gap between the  $\pi$  and the  $\sigma$  (or  $\sigma^*$ ) localized orbitals and is a positive quantity.

Although both  $\sigma$  and  $\sigma^*$  NBOs participate in  $\pi$ -TB coupling, interactions involving the  $\sigma$  NBOs are expected to be dominant, mainly because the  $\pi_{\text{NBO}}/\sigma_{\text{NBO}}$  energy gap (ca. 10 eV) is much smaller than the  $\pi_{\text{NBO}}/\sigma^*_{\text{NBO}}$  energy gap (ca. 25 eV), and also because the  $\sigma$  NBOs are relatively compact and have fewer nodes, compared to the  $\sigma^*$  NBOs. Consequently, our qualitative discussion of  $\pi$ -TB coupling may be satisfactorily confined to interactions involving only  $\sigma$  NBOs.<sup>57</sup>

Interactions between various pairs of  $\sigma$  NBOs in the two relays of the polynorborene and hybrid norbornane-bicyclo[2.2.0]hexane bridges are shown in Scheme 1, together with their average HF/3-21G energies. Two points are noteworthy. Firstly, the through-space interrelay interaction terms,  $t_2-t_6$ , are significantly smaller than the intrarelay interactions  $t_1$  and  $t_{1a}$ , between adjacent  $\sigma$  NBOs; consequently,  $\Delta E(\pi)$  arising from coupling through a single main relay should be larger than that arising from an interrelay pathway, although the large number of the latter paths may well combine to give a sizeable contribution to the overall splitting energy (provided that they have the same parity). Secondly, interrelay jumps of the type  $t_2$  and  $t_3$ , involving NBOs that are directly facing each other within a ring are significantly larger than those interrelay jumps involving other pairs of NBOs, such as  $t_4-t_6$ .

Indeed, calculations carried out on selected systems confirmed that  $\sigma/\sigma$  interactions of the type  $t_4-t_6$  have only a negligible influence on  $\pi$ -TB coupling in the bridges studied here. Consequently, we concentrate only on interrelay pathways that involve through-space jumps between directly facing NBOs, some of which are shown in Figure 1.

We illustrate this analysis by considering the 10-bond polynorborene diene system, **2(10)**, and the 10-bond hybrid norbornane-bicyclo[2.2.0]hexane diene system, **3(10)**. The phases of the localized  $\pi$  and bridge C-C  $\sigma$  basis orbitals are (arbitrarily) chosen such that there are no phase inversions between overlapping pairs of adjacent orbitals. This is shown in Figure 1a for **2(8)**. With this system of orbital phases, all the  $T$  and  $t_1$  interaction elements are negative quantities.

The bridge C-C bonds that are directly attached to the double bonds are not considered in the forthcoming analysis; local planarity about the C=C double bonds ensures that the interaction between the  $\pi$  NBOs and their adjacent C-C  $\sigma$  NBOs are weak (-0.26 eV) compared to the depicted allylic  $T$  interaction (-1.23 eV), and their omission makes little difference to the overall argument. Interrelay pathways involving an odd number of through-space jumps (e.g., Figure 1d and 1e) and pathways proceeding through the ring-fusion cross-link bonds (e.g., Figure 1g) all have odd parity and therefore are predicted to interfere destructively with coupling through the main relays (Figure 1c) which possess even parity. Interrelay pathways involving an even number of through-space jumps (e.g., Figure 1f) have even parity and therefore reinforce the coupling through the main relays, as do interrelay pathways that pass through the methano bridges (Figure 1h). These conclusions are in accordance with the relative signs of the  $\Delta E(\pi)$  values, shown in Figure 1 for the various pathways obtained from the McConnell nearest-neighbor expression, eq 4.

From eq 4, splittings arising from pathways involving  $p$  through-space jumps contain the factor  $(t_2/\Delta)^p$  (assuming that all through-space interactions of the type  $t_2$  are approximately equal, which is borne out by NBO analyses). Since the value

(57) Balaji, V.; Ng, L.; Jordan, K. D.; Paddon-Row, M. N.; Patney, H. *K. J. Am. Chem. Soc.* **1987**, *109*, 6957.

**Table 1.** HF/3-21G  $\pi_+, \pi_-$  Splitting Energies,  $\Delta E(\pi)$ , and  $\pi^*, \pi^*$  Splitting Energies,  $\Delta E(\pi^*)$  (eV), and Corresponding  $\beta_h$  and  $\beta_e$  Values (Per Bond) for **2(n)**, **3(n)**, and **4(n)**

| n         | $\Delta E(\pi)$    |                    |                    | $\Delta E(\pi^*)$  |                    |                    |
|-----------|--------------------|--------------------|--------------------|--------------------|--------------------|--------------------|
|           | <b>2(n)</b>        | <b>3(n)</b>        | <b>4(n)</b>        | <b>2(n)</b>        | <b>3(n)</b>        | <b>4(n)</b>        |
| <b>4</b>  | 1.017              |                    | 0.548              | 0.907              |                    | 0.718              |
| <b>6</b>  | 0.344              | 0.199              | 0.282              | 0.181              | 0.232              | 0.194              |
| <b>8</b>  | 0.151              |                    | 0.160              | 0.0886             |                    | 0.0737             |
| <b>10</b> | 0.0781             | 0.0250             | 0.0961             | 0.0314             | 0.0308             | 0.0356             |
| <b>12</b> | 0.0396             |                    | 0.0580             | 0.0102             |                    | 0.0132             |
| <b>14</b> | 0.0200             | 0.00222            | 0.0351             | 0.00380            | 0.00326            | 0.00498            |
| <b>16</b> | 0.0102             |                    | 0.0214             | 0.00134            |                    | 0.00208            |
|           | $\beta_{h(n,n+2)}$ | $\beta_{h(n,n+4)}$ | $\beta_{h(n,n+2)}$ | $\beta_{e(n,n+2)}$ | $\beta_{e(n,n+4)}$ | $\beta_{e(n,n+2)}$ |
| <b>4</b>  | 0.54               |                    | 0.33               | 0.81               |                    | 0.66               |
| <b>6</b>  | 0.41               | 0.50               | 0.28               | 0.36               | 0.50               | 0.48               |
| <b>8</b>  | 0.33               |                    | 0.25               | 0.52               |                    | 0.36               |
| <b>10</b> | 0.34               | 0.61               | 0.25               | 0.56               | 0.56               | 0.50               |
| <b>12</b> | 0.34               |                    | 0.25               | 0.50               |                    | 0.49               |
| <b>14</b> | 0.34               |                    | 0.25               | 0.52               |                    | 0.44               |

of  $t_2/\Delta$  for through-space jumps in norbornane rings is small ( $-0.12$ ), it follows that single-jump pathways, which involve the factor  $(t_2/\Delta)$ , are more important than double-jump pathways, which involve the factor  $(t_2/\Delta)^2$ , even though there are more of the latter than the former,<sup>40</sup> and the overall result is therefore destructive interference. For example, in the case of **2(10)**, there are 16 different single-jump pathways and 56 different double-jump pathways.<sup>58</sup>

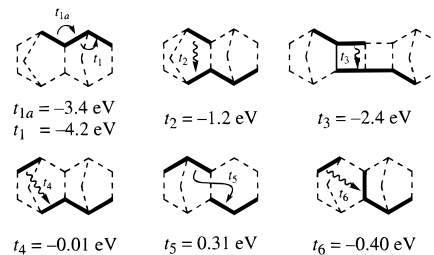
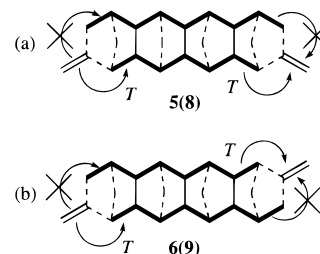
It is important to note that, although the arguments and reasoning presented above concerning the parity rule and its application were discussed in terms of the simple McConnell nearest-neighbor approximation (eq 4), the conclusions are expected to hold true for the exact case in which the full Fock matrix in the basis of the NBOs for a particular pathway is diagonalized. In this case *all* interactions between the  $\pi$  and  $\sigma$  NBOs making up a particular pathway are included in the diagonalization. For example, the exact NBO/3-21G signed  $\Delta E(\pi)$  values for the various pathways for **2(10)** and **3(10)** depicted in Figure 1 are as follows:

|                        |      |      |         |       |
|------------------------|------|------|---------|-------|
| Figure 1 pathway:      | 1c   | 1d   | 1e      | 1f    |
| $\pi$ splitting (meV): | 33.0 | -5.2 | -0.0093 | 0.076 |
| Figure 1 pathway:      | 1g   | 1h   | 1i      | 1j    |
| $\pi$ splitting (meV): | -9.2 | 1.1  | -9.1    | -3.6  |

As can be seen, the signs of the splittings are in agreement with those predicted by the parity rule. As expected, the magnitude of the  $\pi$  splitting energies reflects both the length of the coupling pathways and the magnitude of the NBO interaction elements that form each pathway.

Consideration of interrelay interference nicely explains why the  $\Delta E(\pi)$  and limiting  $\beta_h$  values for the series of dienes **3(n)** are notably inferior to the corresponding values for the series **2(n)** (Table 1). The bridge in the former series consists of both bicyclo[2.2.0]hexane and norbornane units. The absolute magnitudes of the  $t_3$  interrelay interactions within the bicyclo[2.2.0]hexane groups in **3(n)** (Scheme 1) are, on the average, twice as large as the  $t_2$  interactions within the norbornane rings in **2(n)** and **3(n)**. This difference in the magnitudes of  $t_2$  and  $t_3$  is reflected by the  $\Delta E(\pi)$  values for the two types of single jump pathways shown in Figure 1i,j, being  $-9.1$  and  $-3.6$  meV, respectively. Consequently, destructive interference is stronger in the hybrid bridge in **3(n)**, compared to the polynorbornane bridge in **2(n)**. This is an important conclusion because most

(58) The number of single-jump and double-jump pathways given in the text ignores any retracing pathways and pathways involving the terminal bridge  $\sigma$  bonds. See also ref 40.

**Scheme 1****Scheme 2**

of our experimental HT and ET work has been carried out using such hybrid bridges.<sup>9,25-28</sup>

It should be possible to use the parity rule to design bridges in which coupling pathways involving through-space interrelay interactions interfere *constructively* with the coupling through the main relays. Indeed, we have successfully realized this possibility using the following procedure.

We begin by noting that destructive interference in **2(n)** and **3(n)** arises from pathways involving an odd number of interrelay jumps which, by necessity, commence on one main relay and terminate on the other main relay. Since pathways involving an even number of interrelay jumps (e.g., Figure 1f) must have the same parity as the main relay from which they originate and to which they eventually return, then coupling arising from these pathways interferes *constructively* with that arising from the main relays. Consequently, we propose that the successful design of a multistrand bridge displaying overall constructive interference should meet either one or both of the following requirements:<sup>59</sup>

(i) Pathways involving an odd number of interrelay jumps have the same parity as the main relays.

(ii) Either one of the main relays is decoupled from both  $\pi$  orbitals (e.g., Scheme 2a), or each main relay is significantly coupled to only one but different  $\pi$  orbital (e.g., Scheme 2b).

It should be pointed out that requirement (i) is only true if the parity of a pathway is determined by taking into account *both* the number of interacting bonds *and* the number of phase inversions between overlapping orbitals within that pathway. This is an important point which will be discussed in more detail below.

In Scheme 3, the  $C_s$  symmetric dienes, **5(n)**, **7(n)**, **9(n)**, **11(n)**, **13(n)**, and **15(n)**,<sup>60</sup> and their respective  $C_2$  symmetric stereoisomers, **6(n)**, **8(n)**, **10(n)**, **12(n)**, **14(n)**, and **16(n)**, appear to meet the first requirement; all reasonable coupling pathways in the  $C_s$  dienes have even parity, and those in the  $C_2$  dienes have odd parity. Figure 2 illustrates this point for the dienes **5(8)** and **6(9)**.

(59) Another possible requirement for constructive interference may be that coupling through interrelay pathways involving an odd number of interrelay jumps is insignificant. However, this requirement implies that coupling through interrelay pathways involving an *even* number of interrelay jumps would also be negligible. Hence, the coupling through a bridge meeting this requirement should not display *any* significant interrelay interference effects at all.

(60) For the  $C_s$  symmetric dienes of Scheme 3,  $n$  refers to the length of the shorter main relay.

## Scheme 3

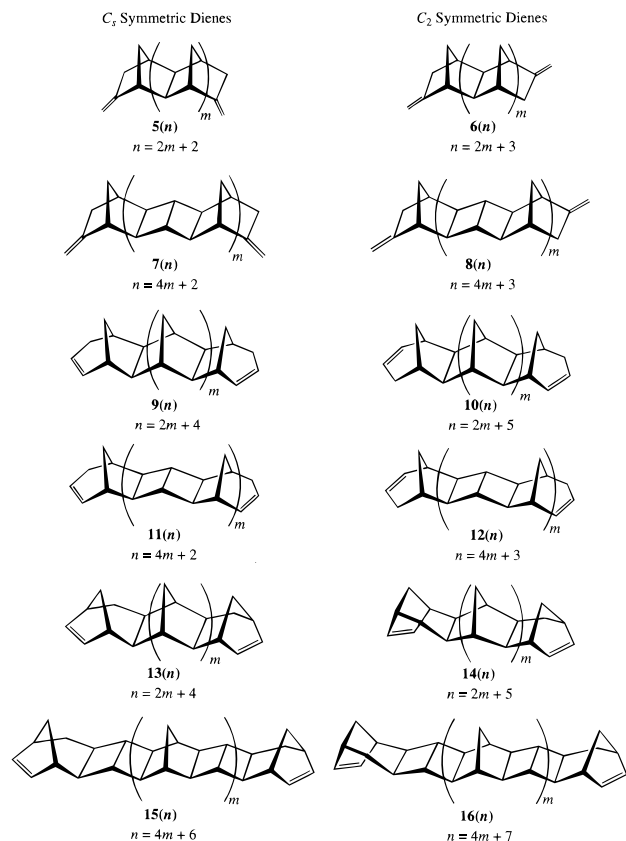


**Table 2.** HF/3-21G  $\pi_+$ - $\pi_-$  Splitting Energies,  $\Delta E(\pi)^a$  (eV), and Corresponding  $\beta_h$  Values (Per Bond) for **5(n)**–**16(n)**

| n         | <b>5(n)</b>        | <b>7(n)</b>        | <b>9(n)</b>        | <b>11(n)</b>       | <b>13(n)</b>       | <b>15(n)</b>       |
|-----------|--------------------|--------------------|--------------------|--------------------|--------------------|--------------------|
| <b>10</b> | 0.138              | 0.263              | 0.135              | 0.246              | 0.145              | 0.219              |
| <b>12</b> | 0.0975             |                    | 0.0927             |                    | 0.0968             |                    |
| <b>14</b> | 0.0689             | 0.211              | 0.0646             | 0.190              | 0.0651             | 0.156              |
| <b>16</b> | 0.0514             |                    | 0.0456             |                    | 0.0440             |                    |
|           | $\beta_{h(n,n+2)}$ | $\beta_{h(n,n+4)}$ | $\beta_{h(n,n+2)}$ | $\beta_{h(n,n+4)}$ | $\beta_{h(n,n+2)}$ | $\beta_{h(n,n+4)}$ |
| <b>10</b> | 0.17               | 0.054              | 0.19               | 0.066              | 0.20               | 0.085              |
| <b>12</b> | 0.17               |                    | 0.18               |                    | 0.20               |                    |
| <b>14</b> | 0.15               |                    | 0.17               |                    | 0.20               |                    |
| n         | <b>6(n)</b>        | <b>8(n)</b>        | <b>10(n)</b>       | <b>12(n)</b>       | <b>14(n)</b>       | <b>16(n)</b>       |
| <b>11</b> | -0.126             | -0.259             | -0.114             | -0.240             | -0.132             | -0.212             |
| <b>13</b> | -0.0918            |                    | -0.0822            |                    | -0.0893            |                    |
| <b>15</b> | -0.0664            | -0.211             | -0.0594            | -0.189             | -0.0611            | -0.156             |
| <b>17</b> | -0.0501            |                    | -0.0429            |                    | -0.0420            |                    |
|           | $\beta_{h(n,n+2)}$ | $\beta_{h(n,n+4)}$ | $\beta_{h(n,n+2)}$ | $\beta_{h(n,n+4)}$ | $\beta_{h(n,n+2)}$ | $\beta_{h(n,n+4)}$ |
| <b>11</b> | 0.16               | 0.052              | 0.17               | 0.059              | 0.20               | 0.076              |
| <b>13</b> | 0.15               |                    | 0.16               |                    | 0.19               |                    |
| <b>15</b> | 0.15               |                    | 0.16               |                    | 0.19               |                    |

<sup>a</sup> A positive (negative) sign for  $\Delta E(\pi)$  indicates a natural (inverted) sequence of  $\pi$  orbitals (see text).

The HF/3-21G  $\Delta E(\pi)$  and  $\beta_h$  values for **5(n)**–**16(n)**, presented in Table 2, confirm our expectation that significant constructive interference is present in these systems. Thus, for the polynorbormane dienes, **5(n)**, **6(n)**, **9(n)**, **10(n)**, **13(n)**, and **14(n)**, the limiting  $\beta_h$  values are approximately one half of that for **2(n)**. The absolute values of  $\Delta E(\pi)$  for the longer members in these series of dienes are also significantly larger than those for the corresponding series **2(n)**, by a factor of three in the case of the 14-bond  $C_s$  systems and the 15-bond  $C_2$  systems.

The results for the hybrid norbornane–bicyclo[2.2.0]hexane bridge dienes, **7(n)**, **8(n)**, **11(n)**, **12(n)**, **15(n)**, and **16(n)**, are even more dramatic; the limiting  $\beta_h$  values for these series are

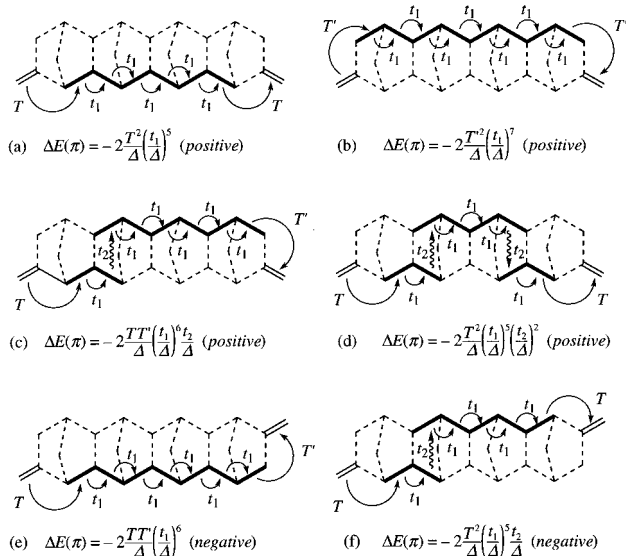
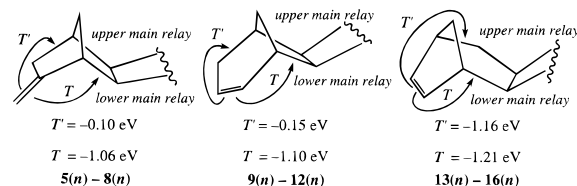


**Figure 2.** Selected TB coupling pathways (highlighted bonds) and McConnell-type nearest-neighbor  $\pi$  splitting energy expressions for the dienes **5(8)** and **6(9)**. See the caption to Figure 1 for general explanatory information.

## Scheme 4



between eight and 12 times smaller than that for **3(n)**, amounting to only 0.052–0.066 per bond for **7(n)**, **8(n)**, **11(n)**, and **12(n)**, and 0.085 and 0.076 per bond for **15(n)**, and **16(n)**, respectively!

The absolute values of  $\Delta E(\pi)$  for the hybrid-bridge dienes **7(14)**, **8(15)**, **11(14)**, **12(15)**, **15(14)**, and **16(15)**, ranging from 0.16 to 0.21 eV, are amazingly large, considering that the two double bonds in these molecules are about 17 Å apart! These  $\Delta E(\pi)$  values are 70 to 95 times larger than that for **3(14)**. The calculated absolute  $\Delta E(\pi)$  splitting of 0.21 eV for both **7(14)** and **8(15)** is large enough to be detectable by photoelectron spectroscopy.

These results are consistent with the comparative analysis of TB coupling in the polynorbormane and the hybrid bridges given above, namely that interrelay interference is stronger in the latter bridge, compared to the former, although it is now manifested as constructive interference in **7(n)**, **8(n)**, **11(n)**, **12(n)**, **15(n)**, and **16(n)**, rather than as destructive interference, as found in **3(n)**. It is noteworthy that the  $\Delta E(\pi)$  and  $\beta_h$  values for **5(n)**–**16(n)** are also markedly superior to those for the single chain system, **4(n)**, thereby confirming that constructive interrelay interactions in these molecules are, indeed, responsible for this improvement.

Examination of the optimized geometries of **5(n)**–**12(n)** reveals that each double bond and one of its associated allylic bridge C–C bonds are essentially coplanar with respect to each other. Consequently, the magnitude of this type of allylic interaction, denoted by  $T'$  in Figure 2 and Scheme 4, should be smaller than that of the other type of allylic coupling, denoted by  $T$ , in which the  $\pi/\sigma$  overlap is greater. Indeed, for **5(n)**–**12(n)**, the NBO/3-21G  $T'$  interaction energy is only ca. -0.12 eV, compared to ca. -1.1 eV for the  $T$  interaction energy (Scheme 4). This analysis leads to the conclusion that, for the  $C_s$  symmetric systems **5(n)**, **7(n)**, **9(n)**, and **11(n)**, one of the

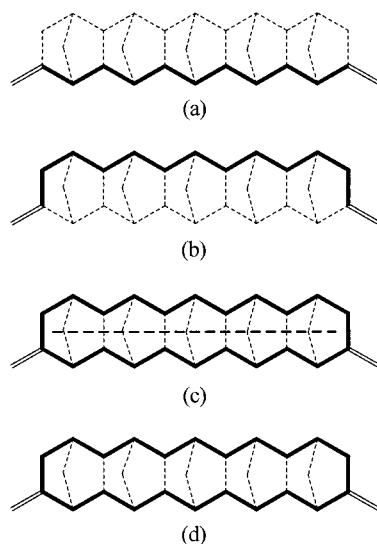


**Figure 3.** Schematic of the various NBO models employed for analyzing TB coupling in **5(10)**. See the text for details.

main relays, namely, the upper one as depicted in these structures, is effectively decoupled from both  $\pi$  NBOs, whereas for the  $C_2$  symmetric dienes, **6(n)**, **8(n)**, **10(n)**, and **12(n)**, each main relay is essentially coupled to only one but different  $\pi$  NBO. These situations are illustrated in Scheme 2 for the case of **5(8)** and **6(9)**. Thus, only interrelay pathways involving an even number of jumps (e.g., Figure 2d) are important in the  $C_s$  series, whereas only pathways involving an odd number of interrelay jumps (e.g., Figure 2f) are important in the  $C_2$  series.

TB coupling through the bridges of these systems was explored further using NBO analysis. The following series of NBO models were applied to the 10- and 12-bond members of the  $C_s$  dienes **5(n)** and **9(n)**.

**Model A.** Only interactions involving the  $\pi$  NBOs and the C–C  $\sigma$  and  $\sigma^*$  NBOs of the lower (i.e., shorter) main relay are included. This relay is strongly coupled to the  $\pi$  NBOs by  $T$  interactions (see Scheme 4). This coupling model is schematized in Figure 3a, for the case of **5(10)**. All other NBO interactions, such as those involving the C–H NBOs, are neglected.

**Model B.** Only interactions involving the  $\pi$  NBOs and the C–C  $\sigma$  and  $\sigma^*$  NBOs of the upper (i.e., longer) main relay are included. This relay is only weakly coupled to the  $\pi$  NBOs. This coupling model is schematized in Figure 3b. All other NBO interactions, such as those involving the C–H NBOs, are neglected.

**Model C.** Interactions involving the  $\pi$  NBOs and the C–C  $\sigma$  and  $\sigma^*$  NBOs of both relays are included. All  $\sigma/\sigma$  and  $\sigma^*/\sigma^*$  interrelay interactions between directly facing NBOs of the two main relays are set equal to zero.<sup>61</sup> This coupling model is schematized in Figure 3c. All other NBO interactions, such as those involving the C–H NBOs, are neglected.

**Model D.** Interactions involving the  $\pi$  NBOs and the C–C  $\sigma$  and  $\sigma^*$  NBOs of both main relays are included. All interrelay interactions between the NBOs of the two relays are retained. This coupling model is schematized in Figure 3d. All other NBO interactions, such as those involving the C–H NBOs, are neglected.

The results of the analysis are presented in Table 3. As expected, restricting TB coupling to the lower main relay (model

(61) Calculations on selected systems revealed that all other interrelay interactions between the  $\sigma$  and  $\sigma^*$  NBOs, such as  $t_4-t_6$  (Scheme 1), have a negligible influence on the  $\pi$  splittings, and so, for convenience, they were retained in model C.

**Table 3.** NBO/3-21G  $\pi_+, \pi_-$  Splitting Energies,  $\Delta E(\pi)$  (eV), and Corresponding  $\beta_h(10,12)$  Values (Per Bond) for **5(n)** and **9(n)**

| NBO model <sup>a</sup> | $\Delta E(\pi)$ |              | $\beta_h(10,12)$ | $\Delta E(\pi)$ |              | $\beta_h(10,12)$ |
|------------------------|-----------------|--------------|------------------|-----------------|--------------|------------------|
|                        | <b>5(10)</b>    | <b>5(12)</b> |                  | <b>9(10)</b>    | <b>9(12)</b> |                  |
| <b>A</b>               | 0.123           | 0.07878      | 0.22             | 0.127           | 0.0802       | 0.23             |
| <b>B</b>               | 0.00005         | 0.00012      | -0.44            | 0.000327        | 0.000348     | -0.03            |
| <b>C</b>               | 0.119           | 0.0742       | 0.24             | 0.118           | 0.0730       | 0.24             |
| <b>D</b>               | 0.279           | 0.260        | 0.03             | 0.253           | 0.236        | 0.03             |

<sup>a</sup> Refer to the text for a description of the NBO models employed.

**A)** gives  $\Delta E(\pi)$  and  $\beta_h$  values for **5(n)** and **9(n)** that are similar to those calculated for the single bridge divinylalkanes **4(10)** and **4(12)** (Table 1). Application of model B leads to no significant coupling at all and this is consistent with the small values of the  $T'$  interactions.<sup>62</sup> Not surprisingly, therefore, incorporating both main relays into the interaction scheme, while omitting interrelay interactions (model C), leads to  $\Delta E(\pi)$  and  $\beta_h$  values that are essentially the same as those calculated using model A.

However, inclusion of interrelay interactions (model D) leads to  $\Delta E(\pi)$  values that are more than doubled in magnitude and to  $\beta_h$  values that are decreased by almost an order of magnitude, compared to the corresponding values calculated using model C! These results clearly confirm the presence of constructive interrelay interference effects in these dienes. Parenthetically, the  $\Delta E(\pi)$  and  $\beta_h$  values calculated using model D are superior to those calculated from the full, HF/3-21G, treatment (Table 2), but this is due largely to the model's neglect of (noninterrelay) pathways involving the C–H bonds, the C–C methano bridge bonds, and the ring-fusion C–C bonds.<sup>63</sup>

In contrast to the case of **5(n)–12(n)**, both  $T$  and  $T'$  interactions have similar magnitudes in **13(n)–16(n)** (Scheme 4), suggesting that TB coupling should be of comparable strength through both upper and lower relays of these systems. It is therefore surprising that the  $\Delta E(\pi)$  and  $\beta_h$  values for **13(n)–16(n)**, which apparently possess two active main relays of the same parity, are somewhat inferior to those for **5(n)–12(n)**, which essentially possess only one active main relay. A series of NBO analyses on the  $C_s$  dienes **13(8)–13(12)** resolved this problem.

NBO models A and B (*vide supra*) were first applied to **13(8)–13(12)** (Table 4). As to be expected, the  $\Delta E(\pi)$  and  $\beta_h$  values for exclusive coupling through the lower main relay of these dienes (model A) are comparable to those calculated for **5(10)–5(12)** using the same model (Table 3). However, the corresponding  $\Delta E(\pi)$  values for exclusive coupling through the upper relay in **13(8)–13(12)** (model B) are markedly inferior to those calculated for the lower relay, even when the difference in length between the upper and lower relay in each diene is taken into account (e.g., compare the  $\Delta E(\pi)$  value for the upper main relay (model B) in **13(8)** with that for the lower main relay (model A) in **13(10)**).

The negligible degree of TB coupling within the upper relay of **13(n)** accounts for the finding that the  $\Delta E(\pi)$  and  $\beta_h$  values obtained using model C are very similar to those obtained using model A. Addition of the interrelay interactions (model D) results in  $\Delta E(\pi)$  increasing 2-fold and to a large decrease in the  $\beta_h$  values, thereby proving that substantial constructive

(62) In fact  $\Delta E(\pi)$  is larger for the 12-bond system than for the 10-bond system in both series, resulting in negative  $\beta_h$  values for this model. However, given the small magnitude of the  $\Delta E(\pi)$  values obtained using model B, this observation probably has little significance.

(63) Results of NBO analyses carried out on the  $C_2$  symmetric dienes **6(n)** and **10(n)** ( $n = 11$  and  $13$ ) also agreed with the qualitative discussion concerning the  $C_s$  symmetric dienes **5(n)** and **9(n)**.

## Scheme 5

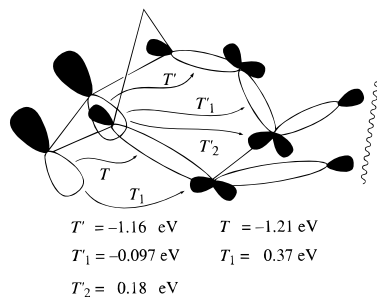


**Table 4.** NBO/3-21G  $\pi_+, \pi_-$  Splitting Energies,  $\Delta E(\pi)$  (eV), and Corresponding  $\beta_h$  Values (Per Bond) for **13(n)**

| NBO model <sup>a</sup> | $\Delta E(\pi)$ |               |               | $\beta_{h(8,10)}$ | $\beta_{h(10,12)}$ |
|------------------------|-----------------|---------------|---------------|-------------------|--------------------|
|                        | <b>13(8)</b>    | <b>13(10)</b> | <b>13(12)</b> |                   |                    |
| <b>A</b>               | 0.198           | 0.123         | 0.0777        | 0.24              | 0.23               |
| <b>A2</b>              | 0.0788          | 0.0513        | 0.0336        | 0.22              | 0.22               |
| <b>B</b>               | 0.00299         | 0.00216       | 0.00153       | 0.16              | 0.17               |
| <b>B2</b>              | 0.0322          | 0.0217        | 0.0146        | 0.20              | 0.20               |
| <b>C</b>               | 0.188           | 0.113         | 0.0691        | 0.25              | 0.25               |
| <b>D</b>               | 0.306           | 0.258         | 0.232         | 0.09              | 0.05               |

<sup>a</sup> Refer to the text for a description of the NBO models employed.

interrelay interference effects, presumably involving an even number of interrelay jumps, are present in **13(n)**.

The reason for the near lack of TB coupling through the upper main relay in **13(8)**–**13(12)** is attributed to the presence of longer range interactions,  $T'_1$  and  $T'_2$ , between the  $\pi$  NBOs and the respective homoallylic and the bishomoallylic C–C  $\sigma$  NBOs of this relay. These interactions, together with their magnitudes, are shown in Scheme 5. Also shown is the longer range interaction  $T_1$  between the  $\pi$  NBO and the homoallylic C–C  $\sigma$  NBO of the lower main relay. All other longer range interactions between the  $\pi$  NBOs and the bridge  $\sigma$  NBOs are much smaller than those shown in Scheme 5 and are ignored.

Carrying out a model B type NBO calculation on the upper main relay of **13(8)**–**13(12)**, but omitting *all* longer range  $\pi/\sigma$  interactions of the type  $T'_1, T'_2, \dots, T'_n$ , resulted in an order of magnitude improvement in the  $\Delta E(\pi)$  values for this relay (Table 4, model B2). Interestingly, carrying out a model A type calculation on the lower main relay of **13(8)**–**13(12)** but omitting *all* longer range  $\pi/\sigma$  interactions of the type  $T_1, T_2, \dots, T_n$ , caused a *deterioration* in the  $\Delta E(\pi)$  values for this relay (Table 4, model A2).

The deleterious effect of the  $T'_1$  and  $T'_2$  interactions on the  $\Delta E(\pi)$  values for **13(n)** may be explained in terms of the TB interaction pathways of the type shown in Figure 4. In these pathways the phases of the basis NBOs are arbitrarily chosen (for convenience) such that there are no phase inversions between adjacent bridge C–C  $\sigma$  NBOs and between the  $\pi$  NBOs and the bridge allylic C–C  $\sigma$  NBOs. In this arrangement, intrabridge nearest-neighbor couplings,  $t_1$ , and the  $\pi/\sigma$  couplings,  $T, T'$ , and  $T_1$  are negative quantities, while the  $\pi/\sigma$  interactions  $T_1$  and  $T_2$  are positive (Scheme 5).

Consider the coupling pathways through the upper main relay, depicted in Figure 4a–c for the case of **13(8)**.  $\Delta E(\pi)$  for pathway (4a) is expected to be positive. In contrast,  $\Delta E(\pi)$  for pathway (4b), in which a  $\pi$ -allylic  $T'$  interaction is replaced by a  $T_1$  homoallylic interaction is expected to be negative because the coupling now passes through an odd number of C–C relay bonds (i.e., seven in this case).  $\Delta E(\pi)$  is also negative for pathway (4c) because, although pathways (4a) and (4c) have the same parity,  $T'$  and  $T_2$  have opposite signs ( $T_2$  is associated

with an out-of-phase overlap between the lower lobe of the  $\pi$  NBO and the rear lobe of the bishomoallylic C–C  $\sigma$  NBO).<sup>64</sup>

Thus, removal of all pathways of the type (4b) and (4c) should lead to a strengthening in TB coupling through the upper main relay, and this is in agreement with the results obtained from model B2.

With regard to TB coupling through the lower main relay,  $\Delta E(\pi)$  is positive for both pathways 4d and 4e because, although the pathways have opposite parities,  $T$  and  $T_1$  have opposite signs. Consequently, removal of pathways of the type (4e) from the interaction scheme should lead to an *attenuation* of TB coupling through the lower main relay, in agreement with the results from model A2.<sup>65</sup>

The analysis of TB coupling in **13(n)** leads to an important conclusion namely, *that the sign of  $\Delta E(\pi)$  for a particular pathway depends not only on the parity of the number of bonds making up the pathway but also on the topology of the orbital overlaps along that pathway.*

This additional complication of orbital overlap topology leads to an extended version of the parity rule for predicting the *relative* signs of  $\Delta E(\pi)$  for two different pathways. This entails calculating for each pathway the sum  $S_i = n_i + p_i$  ( $i = 1, 2$ ), where  $n_i$  is the number of single bonds making up the pathway, and  $p_i$  is the total number of orbital phase inversions between adjacent orbitals along the pathway. If  $S_1$  and  $S_2$  have the same parity, then the  $\Delta E(\pi)$  values for the two pathways have the same sign and the combined TB coupling through both pathways is stronger than that through either pathway (i.e., constructive interference results). On the other hand, if  $S_1$  and  $S_2$  have opposite parity, then the  $\Delta E(\pi)$  values for the two pathways have opposite signs, and the combined TB coupling through both pathways is therefore weaker than that through either pathway (i.e., destructive interference results). This modified parity rule, which we call the *relative parity rule*, permits one to determine whether two coupling pathways will interfere constructively or destructively. Note that the parity of  $S_i$  for a particular pathway depends on the (arbitrary) phases assigned to the basis orbitals making up the pathway.<sup>66</sup> Nevertheless, the *relative* parity of  $S_1$  and  $S_2$  for two pathways is *invariant* to any choice of the phases of the basis orbitals; hence the name *relative parity rule*.

Application of the relative parity rule to the pathways shown in Figure 4 for **13(8)** is straightforward. The  $S_i$  values for pathways (4a), (4b), and (4c) are 8 ( $n_i = 8; p_i = 0$ ), 7 ( $n_i = 7; p_i = 0$ ), and 7 ( $n_i = 6; p_i = 1$ ), respectively, whereas those for (4d) and (4e) are both equal to 6. Thus, the values of  $S_i$  for pathways (4b) and (4c) have opposite parity to that for pathway (4a), whereas the  $S_i$  values for pathways (4d) and (4e) have the same parity. This procedure therefore correctly predicts that TB coupling through the upper main relay in **13(8)**, and in all members of this series, should be inferior to that through the lower main relay.

(64) The  $\Delta E(\pi)$  values for pathways (4a) and (4c) have opposite signs irrespective of how the relative phases of the basis orbitals are chosen. This is because the product  $Tt_1t_1$ , arising from the first three jumps in pathway (4a), and  $T_2$ , arising from the first jump in pathway (4c) (both types of jumps ending at the same point on the main relay) will always have opposite signs.

(65) That the  $\Delta E(\pi)$  values for the two homoallylic pathways (4b) and (4e) have opposite signs is the consequence of geometrically imposed different modes of orbital overlap that exist between the  $\pi$  NBO and the homoallylic bonds. In the case of pathway (4b) the  $\pi$  NBO overlaps with the main lobe of the upper relay homoallylic C–C  $\sigma$  NBO, whereas in the case of pathway (4e) the  $\pi/\sigma$  overlap involves the tail of the lower relay homoallylic C–C  $\sigma$  NBO.

(66) That is, depending on how the phases are assigned to the basis orbitals, it is possible for the parity of the sum,  $S_i$ , calculated for a coupling pathway, to be odd (even), even though the splitting induced by that pathway follows a natural (inverted) sequence.



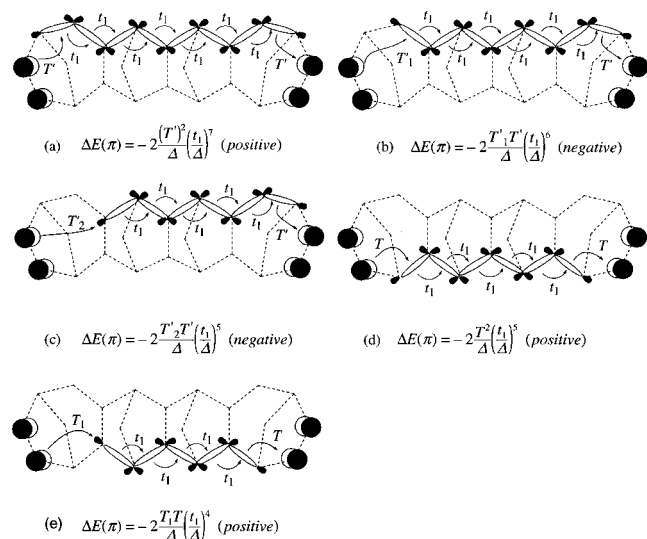


**Figure 4.** Selected  $\pi$ -TB coupling pathways that commence with different  $\pi/\sigma$  jumps in the diene **13(8)**. The sign of the  $T_2$  and  $T_1$  interaction energies is positive, whereas the sign of the  $T'$ ,  $T_1$ , and  $T$  interaction energies is negative. See the caption to Figure 1 for general explanatory information.

**Table 5.** HF/3-21G  $\pi^*_{+}, \pi^*_{-}$  Splitting Energies,  $\Delta E(\pi^*)$  (eV), and Corresponding  $\beta_e$  Values (Per Bond) for **5(n)–16(n)**

| n         | <b>5(n)</b>        | <b>7(n)</b>        | <b>9(n)</b>        | <b>11(n)</b>       | <b>13(n)</b>       | <b>15(n)</b>       |
|-----------|--------------------|--------------------|--------------------|--------------------|--------------------|--------------------|
| <b>10</b> | 0.150              | 0.129              | 0.0544             | 0.0511             | 0.0478             | 0.0523             |
| <b>12</b> | 0.0973             |                    | 0.0392             |                    | 0.0298             |                    |
| <b>14</b> | 0.0673             | 0.0427             | 0.0283             | 0.0177             | 0.0204             | 0.0163             |
| <b>16</b> | 0.0450             |                    | 0.0212             |                    | 0.0141             |                    |
|           | $\beta_{e(n,n+2)}$ | $\beta_{e(n,n+4)}$ | $\beta_{e(n,n+2)}$ | $\beta_{e(n,n+4)}$ | $\beta_{e(n,n+2)}$ | $\beta_{e(n,n+4)}$ |
| <b>10</b> | 0.22               | 0.28               | 0.16               | 0.27               | 0.24               | 0.29               |
| <b>12</b> | 0.19               |                    | 0.16               |                    | 0.19               |                    |
| <b>14</b> | 0.20               |                    | 0.14               |                    | 0.18               |                    |
| n         | <b>6(n)</b>        | <b>8(n)</b>        | <b>10(n)</b>       | <b>12(n)</b>       | <b>14(n)</b>       | <b>16(n)</b>       |
| <b>11</b> | 0.1410             | 0.120              | 0.0399             | 0.0380             | 0.0363             | 0.0437             |
| <b>13</b> | 0.0944             |                    | 0.0343             |                    | 0.0264             |                    |
| <b>15</b> | 0.0650             | 0.0417             | 0.0263             | 0.0163             | 0.0187             | 0.0155             |
| <b>17</b> | 0.0446             |                    | 0.0205             |                    | 0.0135             |                    |
|           | $\beta_{e(n,n+2)}$ | $\beta_{e(n,n+4)}$ | $\beta_{e(n,n+2)}$ | $\beta_{e(n,n+4)}$ | $\beta_{e(n,n+2)}$ | $\beta_{e(n,n+4)}$ |
| <b>11</b> | 0.20               | 0.27               | 0.08               | 0.21               | 0.16               | 0.26               |
| <b>13</b> | 0.19               |                    | 0.13               |                    | 0.17               |                    |
| <b>15</b> | 0.19               |                    | 0.13               |                    | 0.16               |                    |

### Through-Bond Interactions Involving $\pi^*$ Orbitals

We now turn to  $\pi^*$ -TB coupling in the dienes **2(n)–16(n)**, the HF/3-21G  $\Delta E(\pi^*)$  and  $\beta_e$  values for which are presented in Tables 1 and 5. Perusal of these quantities reveals the following salient points:

(1)  $\pi^*$ -TB coupling is significantly weaker than  $\pi$ -TB coupling in the single relay divinylalkanes **4(n)**. For example, for **4(14)**,  $\Delta E(\pi^*)$  is seven times smaller than  $\Delta E(\pi)$  and the limiting  $\beta_e$  value is almost twice as large as the limiting  $\beta_h$  value.

(2) Interrelay destructive interference has less of an effect on  $\pi^*$ -TB coupling than it has on  $\pi$ -TB coupling in both **2(n)** and the hybrid bridge systems **3(n)** (Table 1). Thus, the limiting  $\beta_e$  values for **2(n)** and **3(n)** are, respectively, 18% and 27% larger than that for **4(n)**, whereas the limiting  $\beta_h$  values for **2(n)** and **3(n)** are, respectively, 36% and 144% larger than that for **4(n)**.

(3)  $\pi^*$ -TB coupling in the dienes **5(n)–16(n)** is enhanced by constructive interference (Table 5), although to a diminished extent in some of these systems compared to that found for

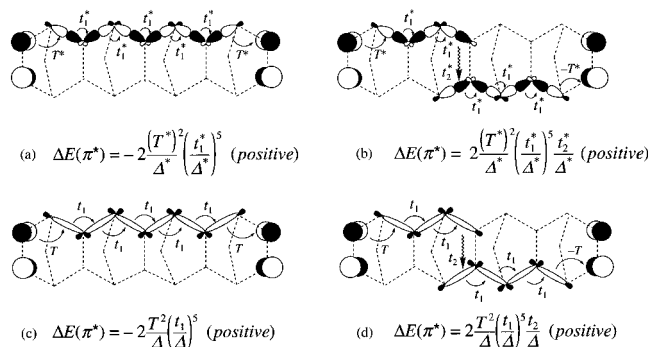


**Figure 5.** Selected  $\pi^*$ -TB coupling pathways through  $\sigma^*$  (a, b) and  $\pi^*$  (c, d) orbitals and McConnell-type nearest-neighbor  $\pi^*$  splitting energy expressions for **2(8)**. Note that  $T$  and  $\Delta$  for (c) and (d) are not the same as those depicted in Figure 1 (which involve  $\pi$  rather than  $\pi^*$  NBOs).

$\pi$ -TB interactions in the same systems. For example, although the limiting  $\beta_e$  values for the polynorbomane bridge systems, **5(n)**, **6(n)**, **9(n)**, **10(n)**, **13(n)**, and **14(n)** (0.13–0.20 per bond) are comparable in magnitude to their corresponding  $\beta_h$  values (0.15–0.20), those for the hybrid bridge systems, **7(n)**, **8(n)**, **11(n)**, **12(n)**, **15(n)**, and **16(n)** are significantly larger (0.21–0.29 per bond) compared to their corresponding  $\beta_h$  values (0.05–0.09 per bond).

(4) The  $\Delta E(\pi^*)$  splitting energies for all the  $C_2$  symmetric dienes of Scheme 3 are *positive* quantities, that is, the symmetric combination,  $\pi^*_{+}$  lies below the antisymmetric combination,  $\pi^*_{-}$  in energy, even though the double bonds are connected by main relays possessing an *odd* number of bonds. We have no convincing explanation for this violation of the parity rule.

Superficially, with the exception of point (4) above, these data are in qualitative agreement with the trends predicted using the parity rule as originally formulated,<sup>1–3</sup> although the small degree of destructive interference present in **2(n)** and **3(n)** may seem at first odd. However, consideration of coupling pathways in these systems using the *relative parity rule* leads to the prediction that  $\pi^*$ -TB coupling in **2(n)** and **3(n)** actually should be *enhanced by constructive interference*, rather than weakened by destructive interference. This is illustrated in Figure 5 for the case of **2(8)** in which coupling of the  $\pi^*$  orbitals through both  $\sigma$  and  $\sigma^*$  relays is considered. Interrelay coupling involving an odd number of jumps (i.e., Figure 5b,d) has the *same* sign as coupling through the main relay (i.e., Figure 5a,c). This may be contrasted with the situation for  $\pi$ -TB coupling (cf. pathways shown in Figure 1a,b). The fact that HF/3-21G calculations reveal that  $\pi^*$  coupling in **2(n)** and **3(n)** is overall weakened by destructive interference, rather than strengthened by constructive interference, will be addressed below.

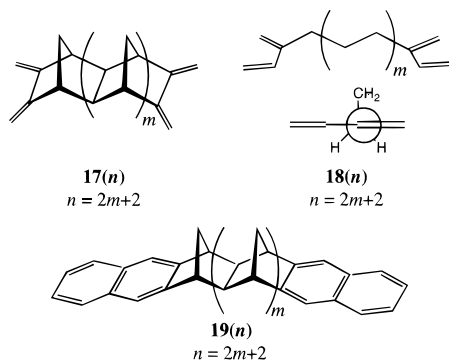
Consideration of the relative parity rule leads to the prediction that  $\pi^*$ -TB coupling in **5(n)–8(n)** should exhibit constructive interference, and this has been found to be the case; the limiting  $\beta_e$  values for **5(n)–8(n)** are substantially smaller than that for **4(n)**. The distance dependence and the magnitude of the splitting energies resulting from  $\pi^*$ -TB interactions in **5(n)** and **6(n)** are similar to those resulting from  $\pi$ -TB interactions. However, this situation is not observed in the case of the hybrid bridge systems **7(n)** and **8(n)**, for which the limiting values for  $\beta_e$  are ca. 0.27 per bond, compared to only ca. 0.05 per bond for  $\beta_h$ . Although the relative parity rule predicts destructive interference for  $\pi^*$ -coupling in **9(n)–16(n)**, the reverse is found. This is because, for reasons given above, the  $\pi^*$  orbitals, like the  $\pi$  orbitals are not coupled to both main relays of the bridge.

Why are  $\pi^*$ -TB interactions weaker than  $\pi$ -TB interactions in **4(n)**, and why is destructive interference, rather than

constructive interference as predicted by the relative parity rule, manifested in  $\pi^*$ -TB coupling in **2(n)** and **3(n)**? Bearing in mind that  $\sigma^*$  orbitals play a dominant role in  $\pi^*$ -TB interactions, but only a minor role in  $\pi$ -TB interactions, the answer to both questions might be that coupling through  $\sigma$  NBOs is stronger than coupling through  $\sigma^*$  NBOs. This explanation suggests that  $\pi^*$ -TB coupling in **2(n)** and **3(n)** should be improved by enhancing the contribution to the coupling made by the  $\sigma$  orbitals. This prediction was verified using a "tuning" procedure,<sup>67</sup> in which the self-energies of the  $\pi^*$  NBOs (ca. 6.4 eV) of selected dienes are set equal to the self-energies for the corresponding  $\pi$  NBOs (ca. -9.95 eV) of the same systems, and diagonalizing the resulting modified Fock NBO matrices to obtain new  $\Delta E(\pi^*)$  values. This  $\pi^*$ -tuning operation ensures that TB coupling involving the tuned  $\pi^*$  orbitals will occur predominantly through the  $\sigma$  orbitals, rather than through the  $\sigma^*$  orbitals of the bridge. This procedure was applied to **2(n)** and **4(n)**, and the data are given in Table 6.

Tuning the  $\pi^*$ -NBO self-energies for **4(n)** leads to a 50% decrease in the limiting  $\beta_e$  value and to a marked increase in  $\Delta E(\pi^*)$ , by nearly an order of magnitude in the case of **4(12)**, compared to the untuned values. The distance dependence of the tuned  $\Delta E(\pi^*)$  values for **4(n)** is nearly the same as that for the corresponding  $\Delta E(\pi)$  values (Table 1).<sup>68</sup> Likewise, there is a substantial improvement in the tuned  $\Delta E(\pi^*)$  and  $\beta_e$  values for **2(n)**, compared to its untuned values.

Constructive interference can therefore play an important role in  $\pi^*$ -TB interactions in bridge systems of the type shown by **2(n)** and, presumably, also in **3(n)**, provided the  $\pi^*$  self-energies are sufficiently low to ensure that the  $\pi^*$ -TB interactions are dominated by coupling through the  $\sigma$  orbitals of the bridge. It is possible to meet this condition in a realistic way using chromophores that possess filled  $\pi$ -type orbitals which are (pseudo)antisymmetric with respect to the (pseudo)plane of symmetry passing through the major molecular axis. For example, the antisymmetric  $\pi$  HOMOs ( $^A\pi$ ) of 1,3-butadienes and 2,3-dialkyl-naphthalenes possess this property, and so one might expect to observe constructive interference effects in systems such as **17(n)** and **19(n)**.



This expectation was verified for the case of **17(n)**, for which the HF/3-21G calculated  $\Delta E(^A\pi)$  and  $\beta_h$  values indicate the presence of strong constructive interference. Thus, the limiting  $\beta_h$  value for **17(n)** was found to be 0.28 per bond, which is 32% smaller than that for the reference single-relay bisbutadienylalkane series **18(n)**, and the  $\Delta E(\pi)$  value for **17(16)** is

(67) Paddon-Row, M. N.; Shephard, M. J.; Jordan, K. D. *J. Am. Chem. Soc.* **1993**, *115*, 3312.

(68) For **4(n)** the  $\pi^*$ -tuned  $\Delta E(\pi^*)$  values are nearly twice as large as their respective HF/3-21G  $\Delta E(\pi)$  values (Table 1). However, this is due to the fact that the absolute magnitude of the interaction matrix element between the  $\pi^*$  NBO and the allylic C-C  $\sigma$  NBO (1.53 eV) is larger than that between the  $\pi$  NBO and the same  $\sigma$  NBO (1.08 eV).

**Table 6.** NBO/3-21G  $\pi^*$ -Tuned  $\pi^*_{+}, \pi^*_{-}$  Splitting Energies,  $\Delta E(\pi^*)^a$  (eV), and Corresponding  $\beta_e$  Values (Per Bond) for **2(n)** and **4(n)**

| n                | $\Delta E(\pi^*)$ |             |
|------------------|-------------------|-------------|
|                  | <b>2(n)</b>       | <b>4(n)</b> |
| <b>4</b>         | 1.518             | 0.736       |
| <b>6</b>         | 0.914             | 0.473       |
| <b>8</b>         | 0.506             | 0.280       |
| <b>10</b>        | 0.292             | 0.174       |
| <b>12</b>        | 0.171             | 0.109       |
| $\beta_e(n,n+2)$ |                   |             |
| <b>4</b>         | 0.25              | 0.22        |
| <b>6</b>         | 0.30              | 0.26        |
| <b>8</b>         | 0.28              | 0.24        |
| <b>10</b>        | 0.27              | 0.24        |

<sup>a</sup> The  $\Delta E(\pi^*)$  and  $\beta_e$  values obtained when the self-energies of the  $\pi^*$  NBO orbitals were altered (tuned) from ca. 6.40 eV to ca. -9.95 eV (i.e., they were set equal to the self-energies of the  $\pi$  NBOs for each system).

0.01 eV, some eight times larger than that for **18(16)** (the full table of data is available as Supporting Information).

### Concluding Remarks

HF/3-21G calculations and NBO analyses of  $\pi$ -TB and  $\pi^*$ -TB coupling through a variety of hydrocarbon bridges linking two double bonds have been carried out. Analysis of the data, together with consideration of the parity rule of TB coupling led to the following important conclusions:

(1) A simple intuitive model, based on the parity rule of TB coupling has been developed that explains interrelay interference effects in TB coupling along various saturated hydrocarbon bridges. The parity rule model was successfully used to design systems **5(n)**–**16(n)** in which the TB coupling between the two double bonds is greatly enhanced by *constructive* interrelay interference.

(2) We have found that constructive and destructive interrelay interference effects can significantly influence the magnitude and distance dependence of TB coupling. For example, the magnitude of  $\Delta E(\pi)$  for the diene **3(14)**, a system in which destructive interrelay interference dominates the  $\pi$ -TB coupling, is 95 times smaller than that for the structurally similar system **7(14)** where constructive interference effects are dominant. Although the magnitude of  $\pi$ -TB coupling arising from a pathway involving interrelay jumps is smaller than  $\pi$ -TB coupling through a main relay, there are many more interrelay pathways than there are main relay pathways, and so the cumulative interrelay coupling can be significant.<sup>69</sup>

(3) The parity rule, in its original form<sup>3</sup> does not take into account any change in parity caused by phase differences between the coupling orbitals within a pathway. Hence, a modified version of the parity rule, which we call the *relative* parity rule, is proposed which takes into account any change in the parity due to the topology of the orbital overlaps along a coupling pathway. The rule is so-named because it only allows the *relative* parities of two pathways to be determined, which is all that is needed for analyzing interference effects in TB interactions.

(4) The relative parity rule works well for  $\pi$ -TB coupling but is less reliable when it is applied to  $\pi^*$ -TB coupling.

(5) The weak distance dependence data for  $\pi$ -TB interactions in the  $C_s$  dienes of Scheme 3 are intriguing since they suggest

(69) For example, most of the sizeable  $\pi$ -TB coupling found in the  $C_2$  symmetric dienes of Scheme 3 is due to interrelay coupling pathways since the  $\pi$  orbitals in these systems are barely coupled to each other through the same main relay.

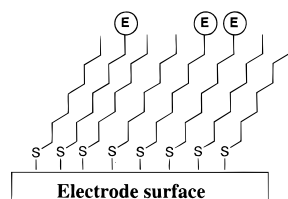


**Figure 6.** Schematic of redox-active-terminated alkanethiol molecules (i.e., those bearing the E label) and diluent alkanethiol molecules adsorbed onto an electrode surface.

that TB coupling through a single hydrocarbon chain may be greatly amplified by a proximate alkane chain which is only weakly coupled, if at all, to the chromophores (e.g., Scheme 2a). Indeed, such amplification may be responsible for some of the small  $\beta$  values that have allegedly been obtained from various experimental electron transfer studies on monolayer assemblies.<sup>70–77</sup> For example, a  $\beta$  value of only 0.007 per bond has been reported for electron transfer in self-assembled monolayers of viologen-terminated alkanecystamines that had been chemisorbed onto gold electrodes.<sup>70</sup> In such instances, amplification of TB coupling within a redox-active-terminated alkanethiol molecule may arise from cooperative through-space interactions (i.e., constructive interference) with alkane chains from neighboring adsorbed molecules, either diluent nonredox-active alkanethiols or other redox-active-terminated alkanethiol molecules (e.g., Figure 6). Admittedly, these chains are not as close to each other as are the two main relays in each of the  $C_s$  dienes of Scheme 3, but this disadvantage is possibly compensated by the presence of many more alkanecystamine chains surrounding each redox system in the monolayer.

(6) The TB coupling data for **5(n)**–**16(n)** are important because they demonstrate that, within the context of Koopmans' theorem, it is possible to design bridges possessing substantially enhanced TB coupling and extremely weak distance dependence characteristics. For example, the calculated  $\Delta E(\pi)$  values for **7(14)** and **8(15)** are two orders of magnitude greater than that

(70) Katz, E.; Itzhak, N.; Willner, I. *Langmuir* **1993**, *9*, 1392.

for **3(14)**, which should translate (using eq 1) into a rate enhancement factor of  $10^4$  for HT in the cation radicals of the former pair of molecules, compared to the cation radical of **3(14)**! However, using simple Koopmans' theorem orbital splitting energies as a measure of the electronic coupling the  $H_e$  (eq 1) should be treated with caution, because, while the KT approximation has been shown to hold well for the series of dienes **2(n)**,<sup>57</sup> there are examples of systems for which the KT calculated splitting energies and  $\beta$  values appear to be, respectively, overestimated and underestimated compared to experimental values.<sup>41,78</sup>

Fortunately, our predictions of extraordinarily large TB coupling in **7(n)**, **8(n)**, **11(n)**, and **12(n)** are amenable to experimental verification since these bridges bearing a variety of chromophores are synthetically accessible. Their syntheses are currently underway.

**Acknowledgment.** M.N.P.-R. thanks the Australian Research Council for continuing support of this research, and M.J.S. acknowledges receipt of a Commonwealth Postgraduate Research Award. Dedicated to Roald Hoffmann on the occasion of his 60th birthday.

**Supporting Information Available:** Table 7 giving the  $\Delta E(\pi)$  and  $\beta_h$  values for **17(n)** and **18(n)** (1 page). See any current masthead page for ordering and Internet access instructions.

JA964132X

- (71) Möbius, D. *Ber. Bunsenges. Phys. Chem.* **1978**, *82*, 848.  
 (72) Kuhn, H. J. *Photochem.* **1979**, *10*, 111.  
 (73) Kuhn, H. J. *Pure Appl. Chem.* **1979**, *51*, 341.  
 (74) Finklea, H. O.; Hanshaw, D. D. *J. Am. Chem. Soc.* **1992**, *114*, 3173.  
 (75) Carter, M. T.; Rowe, G. K.; Richardson, J. N.; Tender, L. M.; Terrill, R. H.; Murray, R. W. *J. Am. Chem. Soc.* **1995**, *117*, 2896.  
 (76) Guo, L.-H.; Facci, J. S.; McLendon, G. *J. Phys. Chem.* **1995**, *99*, 8458.  
 (77) Cheng, J.; Sàghi-Szabó, G.; Tossell, J. A.; Miller, C. J. *J. Am. Chem. Soc.* **1996**, *118*, 680.  
 (78) Curtiss, L. A.; Naleway, C. A.; Miller, J. R. *J. Phys. Chem.* **1993**, *97*, 4050.